0022-3565/05/3143-1370–1377$20.00
THE JOURNAL OF PHARMACOLOGY AND EXPERIMENTAL THERAPEUTICS
Vol. 314, No. 3
87023/3046487
JPET 314:1370–1377, 2005
Printed in U.S.A.

Inhibition of High Voltage-Activated Calcium Channels by Spider Toxin PnTx3-6[S]

Luciene B. Vieira, Christopher Kushmerick,[1] Michael E. Hildebrand, Esperanza Garcia, Antony Stea,[2] Marta N. Cordeiro, Michael Richardson, Marcus Vinicius Gomez, and Terrance P. Snutch

Biotechnology Laboratory, University of British Columbia, Vancouver, British Columbia, Canada (L.B.V., M.E.H., E.G., A.S., T.P.S.); Laboratório de Neurofarmacologia, Departamento de Farmacologia, Instituto de Ciências Biológicas-Universidade Federal de Minas Gerais, Belo Horizonte, Brazil (L.B.V., C.K., M.V.G.); and Centro de Pesquisa Professor Carlos R. Diniz, Fundação Ezequiel Dias, Belo Horizonte, Brazil (M.N.C., M.R.)

Received March 30, 2005; accepted May 31, 2005

ABSTRACT

Animal peptide toxins have become powerful tools to study structure-function relationships and physiological roles of voltage-activated Ca^{2+} channels. In the present study, we investigated the effects of PnTx3-6, a neurotoxin purified from the venom of the spider *Phoneutria nigriventer* on cloned mammalian Ca^{2+} channels expressed in human embryonic kidney 293 cells and endogenous Ca^{2+} channels in N18 neuroblastoma cells. Whole-cell patch-clamp measurements indicate that PnTx3-6 reversibly inhibited L-(α_{1C}/Ca_v1.2), N-(α_{1B}/Ca_v2.2), P/Q-(α_{1A}/Ca_v2.1), and R-(α_{1E}/Ca_v2.3) type channels with varying potency ($\alpha_{1B} > \alpha_{1E} > \alpha_{1A} > \alpha_{1C}$) and IC_{50} values of 122, 136, 263, and 607 nM, respectively. Inhibition occurred without alteration of the kinetics or the voltage dependence of the exogenously expressed Ca^{2+} channels. In N18 cells, PnTx3-6 exhibited highest potency against N-type (conotoxin-GVIA-sensitive) current. In contrast to its effects on high voltage-activated Ca^{2+} channels subtypes, application of 1 μM PnTx3-6 did not affect α_{1G}/Ca_v3.1 T-type Ca^{2+} channels. Based on our study, we suggest that PnTx3-6 acts as a ω-toxin that targets high voltage-activated Ca^{2+} channels, with a preference for the Ca_v2 subfamily (N-, P/Q-, and R-types).

Voltage-activated Ca^{2+} channels play a major role in many physiological processes, including gene transcription, muscle contraction, release of neurotransmitters, and the regulation of neuronal excitability (Catterall, 1995; Dunlap et al., 1995). Furthermore, dysfunction of Ca^{2+} channels is implicated in numerous diseases, including epilepsy, hypertension, chronic pain, migraine, and some arrhythmias (Jen, 1999; Dworakowska and Dolowy, 2000). To find treatments for those diseases, the development of therapeutic Ca^{2+} channel antagonists has been the subject of considerable interest (for review, see Kobayashi and Mori, 1998). As examples, Ziconotide (or Prialt) and AM336, drugs based on the structure of ω-conotoxins, are currently in clinical development for chronic pain management (Schroeder et al., 2004).

The ω-toxins are a family of animal peptide toxins active on Ca^{2+} channels that have become powerful tools for the identification and isolation of Ca^{2+} channel subtypes. The discoveries of ω-conotoxin GVIA, isolated from the venom of a fish-hunting cone shell mollusk and of ω-agatoxin IVA (ω-Aga-IVA), from the spider *Agenelopsis aperta*, aided the identification of N-type (α_{1B}/Ca_v2.2) Ca^{2+} channels and P/Q-type (α_{1A}/Ca_v2.1) Ca^{2+} channels, respectively (Olivera et al., 1985; McDonough et al., 2002). Other examples include the

This work was supported by grants from the Canadian Institute for Health Research (to T.P.S.), a Pronex grant from Fundação de Amparo à Pesquisa do estado de Minas Gerais (Brazil) (to M.V.G.), and a grant from Conselho Nacional de Desenvolvimento Científico e Tecnológico (Brazil) (to M.V.G.) as well the Michael Smith Foundation for Health Research and Natural Sciences and Engineering Research Council of Canada (to M.E.H.). Additional fellowship support was from Coordenação de Aperfeiçoamento de Pessoal de Nível Superior (Brazil) (to L.B.V. and C.K.) and from Conselho Nacional de Desenvolvimento Cientifico e Tecnológico (to L.B.V. and C.K.). T.P.S. is a Senior Investigator of the Canadian Institute for Health Research.

[1] Current address: Departamento de Fisiologia e Biofísica, ICB-Universidade Federal de Minas Gerais, Belo Horizonte, MG, Brazil.

[2] Current address: University-College of the Fraser Valley, Abbotsford, BC, Canada.

Article, publication date, and citation information can be found at http://jpet.aspetjournals.org.

doi:10.1124/jpet.105.087023.

[S] The online version of this article (available at http://jpet.aspetjournals.org) contains supplemental material.

ABBREVIATIONS: ω-Aga-IVA, ω-agatoxin IVA; HVA, high voltage-activated; HEK, human embryonic kidney; TFA, trifluoroacetic acid; HPLC, high-performance liquid chromatography; DMEM, Dulbecco's modified Eagle's medium; LVA, low-voltage-activated; GVIA-S, ω-conotoxin-GVIA-sensitive; GVIA-R, ω-conotoxin-GVIA-resistant; BayK8644, (4*S*)-1,4-dihydro-2,6-dimethyl-5-nitro-4-[2-trifluoromethyl)phenyl]-3-pyridinecarboxylic acid methyl ester; I-V, current-voltage.

inhibition of R-type channels (α_{1E}/Ca_v2.3) by SNX-482, a peptide isolated from the spider *Hysterocrates gigas* (Newcomb et al., 1998), and the inhibition of the T-type channels (α_{1G}/Ca_v3.1 and α_{1H}/Ca_v 3.2) by a scorpion toxin, kurtoxin (Chuang et al., 1998; Sidach and Mintz, 2002).

Toxins isolated from *P. nigriventer* spider venom have been extensively investigated in recent years, and electrophysiological studies indicate diverse effects of different toxins from this venom ranging from activation of Na^+ channels to blockade of K^+ and Ca^{2+} channels (for review, see Gomez et al., 2002). In the present study, we examined PnTx3-6, a member of the PhTx3 fraction (Cordeiro et al., 1993) that includes two other peptides that bind and inhibit HVA Ca^{2+} channels ω-PnTx3-3 (Leão et al., 2000) and ω-PnTx3-4, a peptide essentially identical to the HVA channel blocker ω-phonetoxin IIa (Cassola et al., 1998; Dos Santos et al., 2002).

We have shown previously that PnTx3-6 inhibits K^+-evoked increases in [Ca^{2+}] and Ca^{2+}-dependent glutamate release from synaptosomes (Vieira et al., 2003), suggesting that the toxin targeted Ca^{2+} channels. To characterize the interaction between PnTx3-6 and specific Ca^+ channels as well the potency, selectivity, and possible mechanism of action of the toxin, we studied its effect on recombinant Ca^{2+} channels heterologously expressed in human embryonic kidney (HEK) cells. Moreover, to compare results obtained with cloned Ca^{2+} channels to native neuronal Ca^{2+} channels, we examined the effect of the toxin on Ca^{2+} channel currents recorded from a neuroblastoma cell line, N18 cells, which express both N- and L-type Ca^{2+} channels (Mackie et al., 1993; Carlson et al., 1994).

Materials and Methods

Purification of PnTx3-6. *P. nigriventer* venom was obtained by electrical stimulation of anesthetized spiders. Venom was centrifuged at 4000*g* for 10 min, and the supernatant was fractionated by gel filtration on columns of Sephadex G-50 superfine and superose 12HR, and reverse phase fast protein liquid chromatography on C_2/C_8 (PEP-RPC) and C_1/C_8 (PRO-RPC) columns as described in detail previously (Rezende et al., 1991; Cordeiro et al., 1993). Peptides were detected by monitoring the absorbance at 216 nm (Cordeiro et al., 1993). The fraction PhTx3 obtained from the chromatography on a PRO-RPC column (Rezende et al., 1991) was dissolved in 1 ml of 0.1% (v/v) aqueous trifluoroacetic acid (TFA) and subjected to reverse phase HPLC on a preparative column (22 mm × 25 cm) of Vydac C18 (218TP1022; Technicol Ltd., Stockport, UK) equilibrated in the same solvent. The column was eluted with a linear gradient (0–40% over 180 min) of acetonitrile (HPLC grade S; Rathburn Chemical Co., Peebles, Scotland, UK) in 0.1% TFA at a flow rate of 10 ml min^{-1}. We collected three fractions (A–C; Cordeiro et al., 1993), and fraction C was dissolved in 1 ml of 10 mM sodium phosphate buffer, pH 6.5, and fractionated on a weak cation exchange HPLC column (4.6 mm × 25 cm) of Synchropak CM 300 (Synchrom Inc., Lafayette, IN) equilibrated in the same buffer. After absorption, the columns were eluted with a linear gradient (0–0.5 M NaCl over 90 min) in the same buffer at a flow rate of 2 ml min^{-1}. The toxin PnTx3-6 eluted at a salt concentration of 0.16 M (Fig. 1), and was desalted by absorption onto Sep-Pak C18 cartridges (Waters, Milford, MA), which were then washed with 15 ml of 0.1% TFA, and PnTx3-6 was eluted with 5 ml of acetonitrile containing 0.1% TFA. The purity of PnTx3-6 was assayed using SDS-polyacrylamide gel electrophoresis (16%) and silver staining.

Cell Culture. Human embryonic kidney cells (HEK293 tsA-201) and the neuroblastoma cell line N18 were grown in standard DMEM supplemented with 10% fetal bovine serum, 50 U ml^{-1} penicillin, and 50 μg ml^{-1} streptomycin in a humidified atmosphere of 95% O_2/5% CO_2 at 37°C. N18 cells were mechanically detached in phosphate-buffered saline containing 1 mM EDTA and plated in 35-mm culture dishes. After 1 day, N18 cells were induced to differentiate into the neuronal phenotype by reducing fetal bovine serum to 0.2% and addition of 2% dimethyl sulfoxide (Leão et al., 2000). The culture medium was changed every 2 days and differentiated N18 cells were used within 4 days.

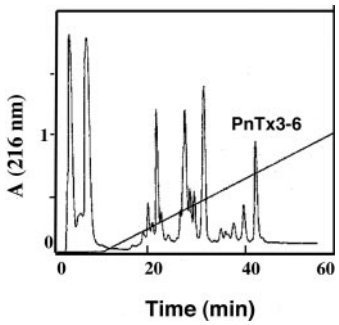

Fig. 1. Chromatogram of the last stage of PnTx3-6 purification (see *Materials and Methods*). The sample was dissolved in 1 ml of 10 mM sodium phosphate buffer, pH 6.5, and applied to a column (4.6 mm × 25 cm) of the weak cation exchanger Synchropak CM 300 equilibrated in the same buffer. The column was eluted with a linear gradient of 0 to 0.5 M NaCl in the same buffer (thick line) at a flow rate of 2 ml min^{-1}. PnTx3-6 was eluting at a salt concentration of 0.16 M NaCl.

Transient Transfection with L-, P/Q-, and R-Type Ca^{2+} Channels. HEK cells were grown to approximately 80% confluence, enzymatically disassociated using 0.25% trypsin in DMEM containing 1 mM EDTA (trypsin/EDTA), plated on 35-mm culture dishes at 5 to 10% confluence, and allowed to recover for 12 h. The medium was then replaced, and the cells were transiently transfected with cDNA plasmids encoding one type of Ca^{2+} channel α subunit [α_{1A} (Starr et al., 1991), α_{1C} (Bourinet et al., 1994), or α_{1E} (Soong et al., 1993)] together with auxiliary subunits β_{1b} and $\alpha_2\delta$ (Zamponi et al., 1997) and CD8 marker plasmid at a molar ratio 1:1:1:0.25 using Lipofectamine (Invitrogen, Carlsbad, CA) following the manufacturer's instructions. After 12 h, the cells were washed with fresh medium, stored at 37°C, and allowed to recover for an additional 36 to 72 h before electrophysiology recordings. Transiently transfected cells were selected for expression of CD8 by adherence of Dynabeads (Dynal, Great Neck, NY).

Generation of Stable Cell Lines Expressing N- and T-Type Ca^{2+} Channels. HEK cells were transfected using linearized cDNA encoding either α_{1G} (McRory et al., 2001) alone or α_{1B} (Dubel et al., 1992) together with β_{1b} and $\alpha_2\delta$ using standard Ca^{2+}-phosphate precipitation, and clones were selected with zeocin. The stable cell lines were enzymatically dissociated using 0.25% trypsin in DMEM containing 1 mM EDTA (trypsin/EDTA), plated on 35-mm culture dishes, and allowed to recover 24 to 36 h before recordings.

Electrophysiological Recordings. Macroscopic currents were recorded using the whole-cell patch-clamp technique (Hamill et al., 1981). Whole-cell currents were recorded using an Axopatch 200A or 200B amplifier (Axon Instruments Inc., Union City, CA), controlled and monitored with a personal computer running pClamp software (Axon Instruments Inc.). Patch pipettes were pulled from borosilicate glass using a PP-830 pipette puller (Narishige, Tokyo, Japan) and had resistances of 2 to 4 MΩ when filled with internal solution. The internal pipette solution contained 120 mM $CsCl_2$, 1 mM $CaCl_2$, 11 mM EGTA, 10 mM HEPES, and 2 mM Mg-ATP, pH 7.2. The bath was connected to ground via a 3 M KCl Agar-bridge. To minimize voltage errors due to series resistances, we discarded cells with whole-cell currents >2 nA. All recordings were performed at room temperature (20–24°C). Signals were low-pass filtered at 2 kHz and sampled at >5 KHz. In some cases, linear leak subtraction was performed using the P/4 protocol included in the Clampex program.

Recordings were analyzed using Clampfit (Axon Instruments Inc.), and off-line leak subtraction was applied to those currents that had not been subtracted on-line. Traces shown in figures were low-pass filtered at 1000 Hz for display. Statistical significance was determined by Student's t tests, and significant values were set as $p < 0.01$ or as indicated in the text and figure legends.

The external recording solution used to measure current through expressed Ca^{2+} channels in HEK cells contained 2 mM $BaCl_2$, 1 mM $MgCl_2$, 10 mM HEPES, 40 mM tetraethylammonium-Cl, 92 CsCl, and 10 glucose, pH 7.4. For recording HVA Ca^{2+} channel current from differentiated N18 cells, we selected round cells with very short neurites to ensure adequate space clamp. These cells often had very small Ca^{2+} channel currents in 2 mM $BaCl_2$ (not shown), and to improve signal to noise, we used a high concentration of $BaCl_2$ compared with HEK cell recordings. The external solution for N18 recordings contained 25 mM $BaCl_2$, 126 mM tetraethylammonium-Cl, 10 mM HEPES, 30 mM $NiCl_2$, 5.4 mM CsCl, 10 mM glucose, and 0.001 tetrodotoxin, pH 7.4.

The time course of Ba^{2+} current inhibition by PnTx3-6 was studied using voltage steps from a holding potential of −100 mV to the peak current potentials obtained from the I-V relationship for each channel type (α_{1A}, −10 mV; α_{1B}, +10 mV; α_{1C}, −5 mV; and α_{1E}: −20 mV). To minimize rundown, these stimuli were applied at frequencies <0.1 Hz. Cells that did not have a stable baseline Ba^{2+} current amplitude or that did not respond to drugs or toxin with a rapid, monophasic change in Ba^{2+} current amplitude were not considered for analysis. Control experiments (in which control perfusion was run for several minutes) indicated that under these conditions, rundown of Ba^{2+} currents was negligible.

To construct conductance-voltage curves, the conductance (G) as a function of test potential (V_{test}) was calculated as

$$G = I/(V_{test} - V_R), \quad (1)$$

where I is the peak current generated by the step depolarization to V_{test}, and V_R is the current reversal potential determined from the I-V relationship. Deactivation was examined through analysis of tail currents after brief depolarizing steps. Steady-state inactivation curves were obtained by applying test depolarization to peak current potentials at the end of 10-s prepulses ranging in voltages from –110 to +20 mV in 10-mV increments.

N18 neuroblastoma cells express N-type (i.e., ω-conotoxin-GVIA-sensitive) and L-type (i.e., dihydropyridine-sensitive) Ca^{2+} channels (Mackie et al., 1993; Carlson et al., 1994). We measured whole-cell Ba^{2+} currents from these cells in the presence of 1 μM tetrodotoxin to block Na^+ channels and Ni^{2+} (30 μM) to inhibit LVA channels. Under these conditions, the fraction of total Ba^{2+} current that was N-type was defined as that inhibited by 1 μM ω-conotoxin-GVIA (Randall and Tsien, 1995) and will be referred to as the GVIA-sensitive (GVIA-S) component. The remaining Ba^{2+} current (resistant to ω-conotoxin-GVIA; GVIA) was partially inhibited by nifedipine (10 μM; not shown) and increased by 5 μM BayK8644 indicating, as expected (Carlson et al., 1994), that it contained L-type current. As described under *Results*, we estimated inhibition of N-type current by PnTx3-6 by comparing inhibition by PnTx3-6 of the total current (GVIA-S and GVIA-R component) with inhibition of the isolated GVIA-R component.

Solutions and Drugs. Stock solutions of PnTx3-6 were prepared in distilled water and stored at –20°C. Toxin was thawed shortly before the experiments and diluted into the bath solution at the appropriate concentration. Bovine serum albumin (0.025%; Jackson Immunoresearch Laboratories Inc., West Grove, PA) was included in all external solutions (both for experiments with HEK cells as well as N18 cells) to avoid nonspecific binding of the toxin. For experiments with expressed Ca^{2+} channels, the perfusion system consisted of a custom-made multiple solution perfusion manifold with four input and four output capillary tubes (custom microfil, 28-gauge, 250-μm inner diameter and 350-μm outer diameter; WPI, Sarasota, FL) ensheathed in a glass pipette. High chemical-resistant Tygon Chemfluor FEP (Norton Performance Plastics, Akron, OH) and Silastic (Fisher Scientific, Nepean, ON, Canada) tubing was used to connect the perfusion manifold to the syringe valve. Perfusion was driven by gravity and adjusted to approximately 0.4 ml min^{-1}. The outputs of the manifold were placed within proximity of the cell, resulting in rapid solution exchange times (<1 s). In experiments with N18 cells, drugs and toxins were bath applied using rapid perfusion of the bath with solution exchange times of <10 s ω-conotoxin-GVIA was purchased from Peptides (Osaka, Japan). All other reagents were of analytical grade.

Results

Purification and Sequence Comparison of PnTx3-6. Figure 1 shows the HPLC profile of the venom fraction from which PnTx3-6 was isolated (for details, see *Materials and Methods*). The sequence of PnTx3-6 presents little similarity to other known peptide toxins. In Table 1, we present the sequence of PnTx3-6 aligned with other peptide toxins exhibiting some sequence similarity and with known activity on vertebrate HVA Ca^{2+} channels. One of these, ω-phonetoxin IIa, was also isolated from *P. nigriventer* venom and potently inhibits rat L- and N-type currents in β cells and dorsal root ganglion neurons, respectively (Cassola et al., 1998), as well as heterologously expressed P/Q-, N-, and R-type currents (Dos Santos et al., 2002). The ω-Aga toxins IIIA and IIIB, which inhibit vertebrate HVA Ca^{2+} channels (Mintz, 1994; Yan and Adams, 2000; McDonough et al., 2002), exhibit 27% (15 amino acids) and 25% (14 amino acids) identity with PnTx3-6, respectively. Much of the identity among these toxins is due to the large number of cysteine residues, a common feature of animal peptide toxins as first described for the conotoxins (Olivera et al., 1985).

PnTx3-6 Selectively Blocks High Voltage-Activated Ca^{2+} Channels. Whole-cell patch-clamp recordings were performed on HEK cells transfected with cDNA coding for one type of Ca^{2+} channel α subunit (α_{1A}, α_{1B}, α_{1C}, or α_{1E}) together with $\alpha_2\delta$ and β_{1b} subunits. Figure 2 shows the

TABLE 1
Sequence alignment of PnTx3-6 with other spider toxins active on vertebrate HVA Ca^{2+} channels
Identical amino acids are shown in bold.

	1
PnTx3-6	A**C**I**C**PR**G**E**C**T . . . **DDCECC**G CDNQ**C**Y**C**PPG SSLGIFK**CSC** . . . AHANKY
ω-Phonetoxin-IIA	S**C**INV**G**DF**C**D GKK**DDCQCC**R DNAF**CSCS**VI FGY.KTN**CR**C EVGTTATSYG
ω-AgaIIIA	S**C**IDI**G**GD**C**D GEK**DDCQCC**R RNGY**CSCY**SL FGYLKSG**CK**C VVGTSAEFQG
ω-AgaIIIB	S**C**IDF**G**GD**C**D GEK**DDCQCC**R SNGY**CSCY**SL FGYLKSG**CK**C EVGTSAEFRR
	51
PnTx3-6	F**C**NR**K**KE**K**CK KA. . . . .
ω-Phonetoxin-IIA	I**C**MA**K**H.**K**CG RQTTCTKPCLS KRCKKNH
ω-AgaIIIA	I**C**RR**K**ARQCY NSDPDK.CES HNKPKRR
ω-AgaIIIB	I**C**RR**K**AKQCY NSDPDK.CVS VYKPKRR

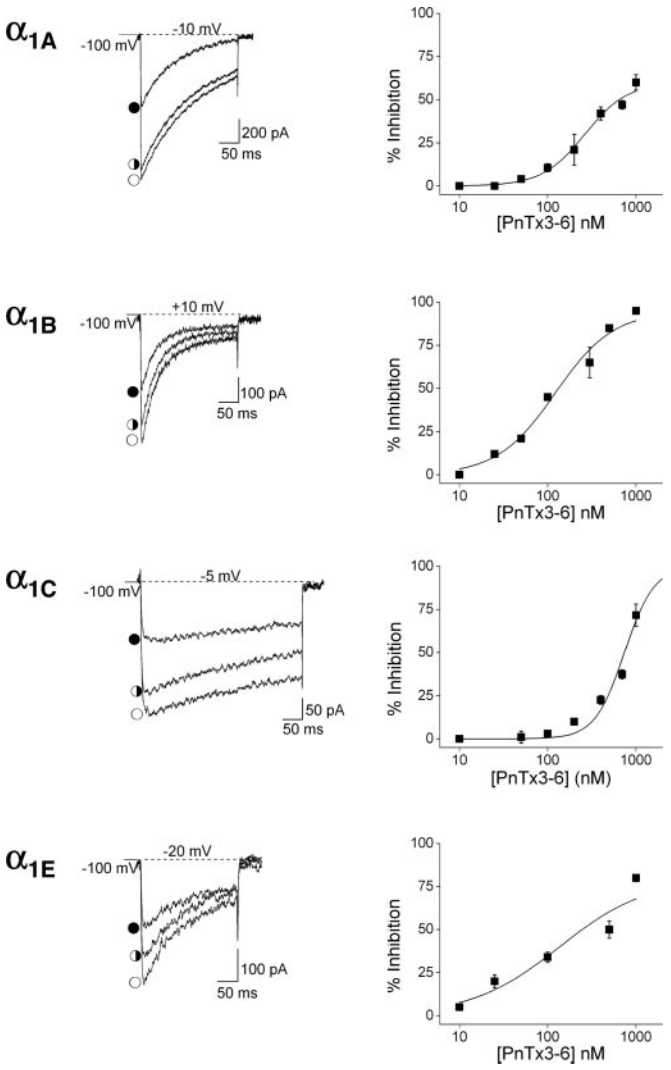

Fig. 2. Reversible and dose-dependent inhibition of cloned HVA Ca^{2+} channels by PnTx3-6. Left, representative current recorded in control (open circles), during the application of PnTx3-6 (filled circles), and after washout of the toxin (semifilled circles). Peak currents were measured during step depolarizations from a holding potential of –100 mV to the peak current potentials obtained from the I-V relationship for each channel type (α_{1A}, −10 mV; α_{1B}, +10 mV; α_{1C}, −5 mV; and α_{1E}, −20 mV). The dose of toxin used in these examples was 500 nM for α_{1A} and α_{1C} and 100 nM for α_{1B} and α_{1E}. Right, dose-response curves for PnTx3-6 inhibition of HVA Ca^{2+} channels. The smooth lines represent fits of the Hill equation: $I = I_{max}/\{1 + (IC_{50}/[PnTx3\text{-}6])^n\}$, where I is the observed percentage of inhibition at a given concentration of toxin, I_{max} is the predicted maximal inhibition, and the Hill coefficient (n) gives a measure of the steepness of the curve. Data points represent mean ± S.E.M. of four to seven independent measurements.

dose-dependent block of the resulting Ba^{2+} currents by PnTx3-6. The toxin produced a reversible block of all four HVA Ca^{2+} channel subtypes tested, although the potency and rate of reversal of inhibition varied among the subtypes (Fig. 2). The effect of PnTx3-6 was dose-dependent, with IC_{50} values of 263 nM for α_{1A}, 122 nM for α_{1B}, 607 nM for α_{1C}, and 136 nM for α_{1E}. The highest concentration of PnTx3-6 used in this study (1 μM) did not produce total block of α_{1A}, α_{1C}, or α_{1E} channels (60, 72, and 80%, respectively; four to seven determinations). However, α_{1B} currents were almost completely blocked (>95%) by this dose. Similar experiments were performed using cloned $\alpha_{1G}/Ca_v3.1$ channels to investigate whether the toxin had affect on LVA T-type channels; however, no effect was observed at a dose of 1 μM PnTx3-6 (Supplemental Fig. 1). Apparent Hill coefficients were close to 1 for block of α_{1A}, α_{1B}, and α_{1E} (1.6, 0.8, and 1.3, respectively). The corresponding value for α_{1C} was 2.6, but we note that this value is poorly constrained because of the low affinity of PnTx3-6 for this channel. For the analysis of blocking kinetics that follows, we assumed a 1:1 interaction between toxin and Ca^{2+} channel.

PnTx3-6 Reversibility and Blocking Kinetics. Figure 3 shows the kinetics of block of the four HVA channel types by different concentrations of PnTx3-6. As expected for a pseudo first-order process, the time course for the development of blockade was accelerated with increasing toxin dose. At each concentration tested, the kinetic of block was well fitted by a single exponential (Fig. 3), and the rate constant

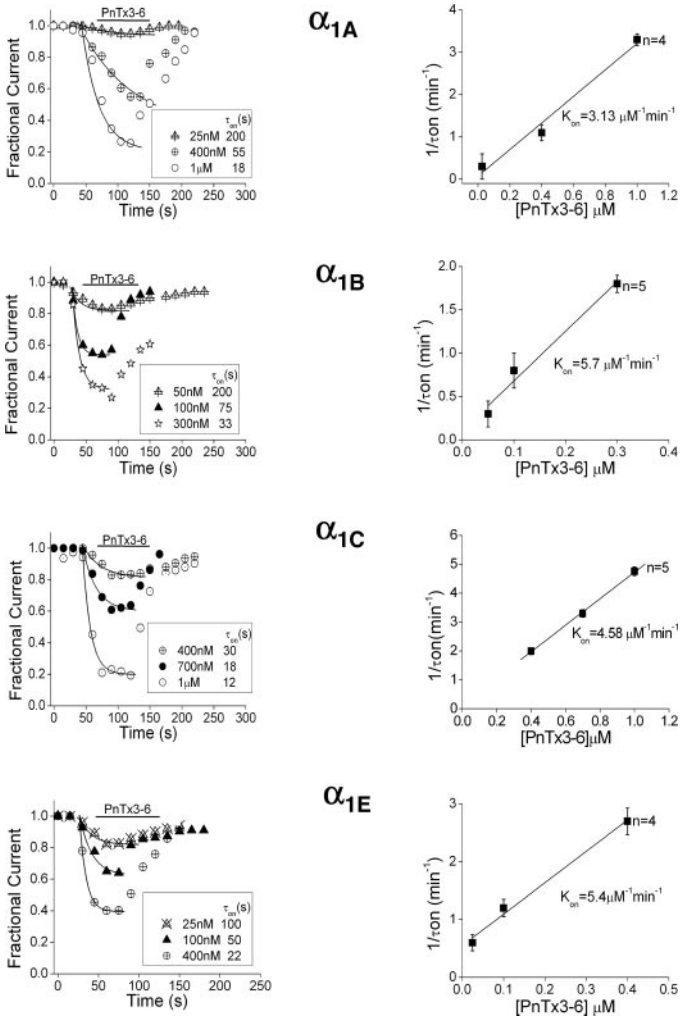

Fig. 3. PnTx3-6 blocking kinetics in HEK 293 cells. Left, representative time courses of development and recovery from block by PnTx3-6. Currents were elicited by stepping from a holding potential of –100 mV to peak current potential (α_{1A}, −10 mV; α_{1B}, +10 mV; α_{1C}, −5 mV; and α_{1E}, −20 mV). In all cases, the block developed more rapidly at higher toxin concentrations. The solid lines are single exponential fits used to determine τ_{on}. Right, reciprocal of the time constant for development of block is plotted versus toxin concentration. Lines represent linear regressions of the data. The slopes of the regression lines were used to estimate values of K_{on}, and the y-intercepts to estimate values of K_{off}. The values of K_{off} thus obtained were 0.07, 0.1, 0.15, and 0.55 min^{-1} for unblock of α_{1A}, α_{1B}, α_{1C}, and α_{1E} channels, respectively.

for development of block was related linearly to toxin concentration with the slope giving a rate constant for toxin binding (K_{on}) of 3.13 ± 0.4 μM^{-1} min^{-1} (n = 4; α_{1A}), 5.7 ± 0.8 μM^{-1} min^{-1} (n = 5; α_{1B}), 4.58 ± 0.15 μM^{-1} min^{-1} (n = 5; α_{1C}), and 5.4 ± 0.1 μM^{-1} min^{-1} (n = 4; α_{1E}). The unblocking rate constants (K_{off}) were obtained from the same sets of data by extrapolating back to [PnTx3-6] = 0 (Fig. 3). The dissociation constants (K_d) calculated from the ratio of the off-rate and on-rate were K_d = 22.4 nM (α_{1A}), K_d = 17.5 nM (α_{1B}), K_d = 33 nM (α_{1C}), and K_d = 102 nM (α_{1E}). The K_d values for α_{1A}, α_{1B}, and α_{1C} channels were different from the IC_{50} values obtained from the dose-response curves, whereas for α_{1E} channels, the two values were similar. Nonetheless, both IC_{50} values and K_d values indicate that PnTx3-6 is most active against channels containing the α_{1B} subunit.

PnTx3-6 Does Not Affect the Voltage Dependence or Kinetics of HVA Ca^{2+} Channels. We examined the voltage dependence and kinetics of current activation, inactivation, and deactivation for the expressed Ca^{2+} channels to determine whether PnTx3-6 modified these biophysical parameters (Figs. 4 and 5; Table 2). In control, half-maximal activation occurred at −17.4 ± 0.3 mV for α_{1A} (n = 8), −2.1 ± 0.1 mV for α_{1B} (n = 5), −17.9 ± 0.3 mV for α_{1C} (n = 6), and −30 ± 1.0 mV for α_{1E} (n = 10). After reduction of the current by 50% with PnTx3-6, these parameters were unchanged: −17 ± 0.5, −2.1 ± 0.4, −17.2 ± 0.2, and −27 ± 3.0 mV, respectively; $p > 0.5$ for all channel types (Fig. 4).

Steady-state inactivation of the HVA Ca^{2+} channel types was studied by applying 10-s prepulses to different membrane potentials before a test pulse to evoke current in control, and after reduction of current by approximately 50% with PnTx3-6 (Fig. 5). Control currents were half-inactivated by such prepulses at potentials of −63 ± 0.5 (α_{1A}; n = 5), −37.5 ± 1.5 (α_{1C}; n = 6), −74 ± 0.5 (α_{1E}; n = 6), and −81.5 ± 0.5 mV (α_{1B}; n = 7), and these values were unchanged by PnTx3-6: −62.5 ± 0.4, −38 ± 1.8, −74 ± 0.7, and −79.6 ± 1.4 mV, respectively; $p > 0.5$ for all channel types.

To further characterize the effect of PnTx3-6 on the kinetics of cloned Ca^{2+} channels, we also analyzed the time constant of activation, inactivation, or deactivation of the four channels tested when the toxin was applied to the cells. Activation and inactivation rate were obtained by fitting exponentials to the rising or decaying phase of currents obtained using the voltage protocols as described for Fig. 2. Deactivation was measured as the decay of current after return to –100 mV after a brief depolarization, as shown in Supplemental Fig. 2. We found that current inhibition by PnTx3-6 was not accompanied by any change in Ca^{2+} channel kinetics (Table 2).

PnTx3-6 Blocks N-Type Currents in N18 Cells. The results above suggest that, of the expressed Ca^{2+} channel types tested, PnTx3-6 inhibited N-type current with the greatest potency and lowest IC_{50}. Previous studies on a different toxin (kurtoxin; Chuang et al., 1998) have described discrepancies between toxin effects on expressed channels and native channels in neurons (Sidach and Mintz, 2002). To examine inhibition of native N-type channels by PnTx3-6, we used N18 neuroblastoma cells, which express L- and N-type HVA Ca^{+} channels (Mackie et al., 1993; Carlson et al., 1994). Na^{+} currents in these cells were blocked with 1 μM tetrodotoxin, and an apparent LVA Ca^{2+} channel current we sometimes observed was blocked with 30 μM $NiCl_2$ (not shown). Under these conditions, PnTx3-6 (200 nM) rapidly inhibited the total whole-cell Ba^{2+} current by 66 ± 5.5% (n = 10; Fig. 6A). No run-down was observed in these cells before addition of toxin, and inhibition induced by the toxin was partially reversible (Fig. 6B). We next measured the amount of N-type current in these cells as the fraction sensitive to inhibition by ω-conotoxin-GVIA (1 μM; Fig. 6C). This GVIA-S component amounted to 41 ± 7.0% of the total current (Fig. 6D).

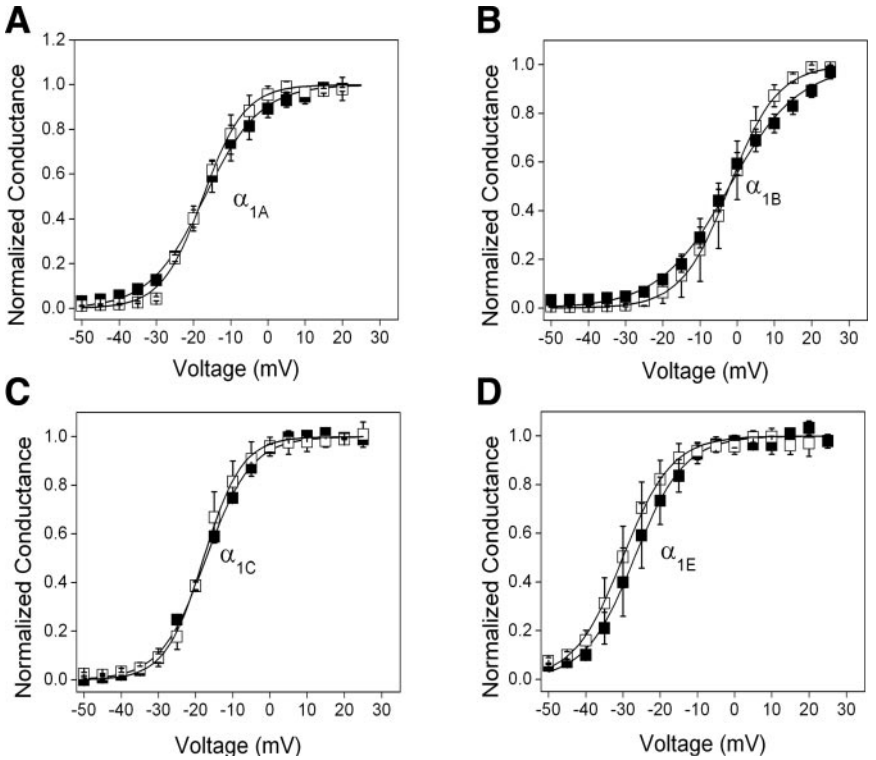

Fig. 4. Voltage dependence of activation of Ca^{2+} channels is not affected by PnTx3-6. Currents were elicited by step depolarizations to the indicated test potentials from a holding potential of –100 mV in control (open symbols) or during approximately 50% inhibition by PnTx3-6 (filled symbols). The toxin concentration used was 500 nM for α_{1A} and α_{1C} (A and C) and 100 nM for α_{1B} and α_{1E} (B and D). Shown are normalized peak conductance as a function of test potentials in control (open symbols) and during for each channel type (A, α_{1A}; B, α_{1B}; C, α_{1C}; and D, α_{1E}). Data were fit with a Boltzmann equation $G/G_{max} = [1 + \exp(\{V - V_a\}/k)]^{-1}$, where G/G_{max} is the normalized peak conductance occurring during a depolarization to the potential V, V_a is the half-activation potential, and k is the slope factor for activation. No effect of PnTx3-6 on the G-V relationship was detected for any of the four channel types tested. Results of the curve fits are given in the text.

TABLE 2
Effects of PnTx3-6 on the kinetics of Ca^{2+} channels
Averages were compiled from different cells, where in parentheses are shown the number of cells. Mean values (± standard error).

Ca Channel	Treatment	τ_{act}	τ_{inact}	τ_{deact}
			msec	
α_{1A}	Ctrl	1.9 ± 0.3 (11)	103 ± 5.2 (11)	0.3 ± 2.0 (11)
	500 nM PnTx3-6	1.7 ± 1.3 (7)	91.5 ± 7.0 (7)	0.4 ± 1.0 (7)
α_{1B}	Ctrl	2.5 ± 0.8 (13)	74 ± 1.5 (13)	0.5 ± 1.2 (13)
	100 nM PnTx3-6	2.1 ± 1.5 (7)	78 ± 2.0 (7)	0.8 ± 0.6 (8)
α_{1C}	Ctrl	2.8 ± 2.4 (15)	183 ± 0.8 (15)	0.4 ± 1.2 (15)
	500 nM PnTx3-6	2.7 ± 1.3 (8)	178 ± 6.0 (8)	0.6 ± 0.8 (8)
α_{1E}	Ctrl	1.1 ± 0.4 (10)	204 ± 5.0 (10)	1.1 ± 0.3 (10)
	100 nM PnTx3-6	1.4 ± 0.2 (7)	208 ± 1.4 (8)	1.06 ± 0.5 (7)

Ctrl, control. There were not significant differences between the cells and treated ($p > 0.05$) in all cases above.

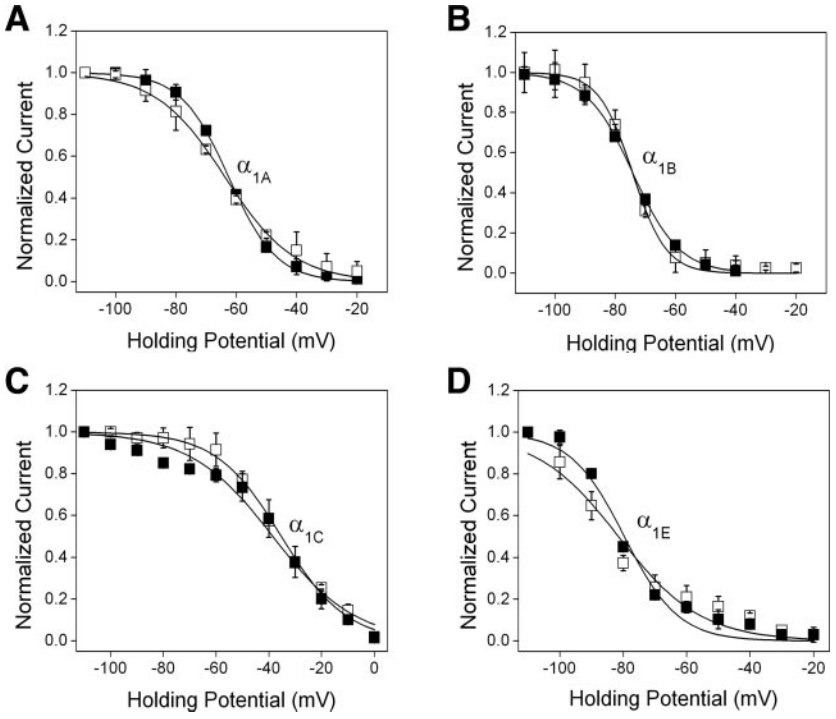

Fig. 5. The voltage dependence of steady-state inactivation of Ca^{2+} channels is not affected by PnTx3-6. Cells were voltage clamped at the indicated prepulse potentials for 10 s and then stepped to the peak current potential for each channel type (α_{1A}, −10 mV; α_{1B}, +10 mV; α_{1C}, −5 mV; and α_{1E}, −20 mV) in control (open symbols) or during approximately 50% inhibition by PnTx3-6 (filled symbols). The toxin concentration used was 500 nM for α_{1A} and α_{1C} (A and C) and 100 nM for α_{1B} and α_{1E} (B and D). Currents during the test pulse were normalized to the current obtained after a prepulse to –120 mV and fit with a Boltzmann equation $G/G_{max} = [1 + \exp(\{V - V_i\}/k)]^{-1}$, where G/G_{max} is the normalized peak conductance occurring during a depolarization to the potential V, V_i is the half-inactivation potential, and k is the slope factor for inactivation. No effect of PnTx3-6 on the steady-state I-V relationship was detected for any of the four channel types tested. Results of the curve fits are given in the text.

BayK8644 increased the remaining GVIA-R component, indicating it contained L-type current (Fig. 6C). PnTx3-6 inhibited the GVIA-R current by 44 ± 7.2%, which was less than the inhibition of the total current (compare Fig. 6, B and E) indicating that ω-conotoxin-GVIA occluded part of the effect of PnTx3-6. Since PnTx3-6 blocked both the GVIA-S and GVIA-R components of the current, the total block (B_T) may be written as

$$B_T = B_S f_S + B_R f_R \quad (2)$$

where B_S and B_R are the amount of Block of the GVIA-S and GVIA-R components, and f_S and f_R are the fraction of the total current represented by each type of component. We measured B_T (66%), f_S (41%), B_R (44%), and f_R (=1 − f_s; 59%), permitting calculation of B_S. We conclude that 200 nM PnTx3-6 inhibits N-type currents in N18 cells by ~98% (Fig. 6F). This determination is only approximate due to the uncertainty in each of the values used to solve eq. 2. Nonetheless, it seems clear that the toxin strongly inhibits the N-type currents and partially inhibits the remaining current natively expressed in N18 cells.

Discussion

PnTx3-6 Inhibition of L-, N-, R-, and P/Q-Type Currents. The present data show PnTx3-6 blockade of mammalian Ca^{2+} channels exogenously expressed in HEK cells, whereas under the same conditions, an LVA (T-type) Ca^{2+} channel ($Ca_v3.1/\alpha_{1G}$) was not affected. Of the four HVA Ca^{2+} channels examined in the study, blockade by PnTx3-6 was most potent and effective on N-type (α_{1B}) Ca^{2+} channels (K_d = 17.5 nM and blockade >95%). In addition to the blockade of N-type channel, PnTx3-6 partially inhibited in a reversible manner current through α_{1A}, α_{1C}, and α_{1E} channels; however, the maximal concentration applied of PnTx3-6 did not block 100% of these channels. The fact that we did not obtain complete blockade of α_{1A}, α_{1C}, and α_{1E} currents may be associated with a state-dependent affinity between the channel and the toxin. As has been previously shown, a number of blockers of voltage-activated Ca^{2+} channels display state and/or holding potential-dependent block (Bean, 1984; Kokubun et al., 1986; Feng et al., 2003; Hildebrand et al., 2004). However, further experiments will be required to deter-

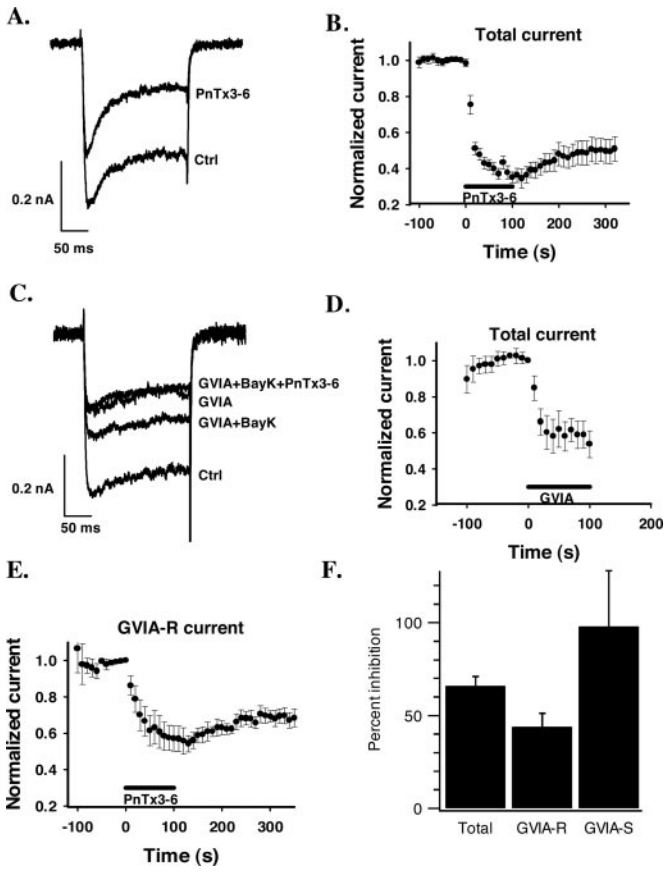

Fig. 6. Inhibition of native HVA Ca^{2+} channel current in N18 cells by 200 nM PnTx3-6. External solution contained 1 μM tetrodotoxin and 30 μM $NiCl_2$. The current traces shown were elicited by voltage steps from a holding potential of −80 mV to +10 mV for 200 ms. The time courses of toxin action were obtained by normalizing the current amplitude for each cell to the amplitude at the time of toxin addition. Each point represents the mean ± S.E. value of the normalized data. A and B, inhibition of total whole-cell Ba^{2+} current by PnTx3-6. A, representative Ba^{2+} current in control and after inhibition with PnTx3-6. B, time course of inhibition of total current by PnTx3-6 (n = 10 cells). C to F, separation of effect of PnTx3-6 on N-type GVIA-S and GVIA-R components of the total Ba^{2+} current. C, representative currents recorded during sequential addition of ω-conotoxin-GVIA (GVIA; 1 μM), BayK4866 (BayK; 5 μM), and PnTx3-6 to the external solution. D, time course of inhibition of the total Ba^{2+} current by ω-conotoxin-GVIA. E, time course of inhibition of the GVIA-R component of the total Ba^{2+} current by PnTx3-6. F, observed inhibition of the total Ba^{2+} current and the GVIA-S component and deduced inhibition of the GVIA-R component by PnTx3-6.

mine whether PnTx3-6 blockade depends on the channel state and/or holding potential-dependent block.

Endogenous Ca^{2+} channel currents have been described previously in HEK cells (ISr-HEK; Berjukow et al., 1996). Such currents were rare (15–20% of cells tested) and very small in the cells that displayed such current (0.39 pA pF^{-1} using 10 mM Sr^{2+} as the charge carrier). In our experiments with HEK cells, we used 2 mM Ba^{2+} as the charge carrier, and this lower concentration of divalent charge carrier may result in even smaller endogenous currents through any putative endogenous channels. We have occasionally seen endogenous currents in HEK cells (M. E. Hildebrand and E. Garcia, unpublished observations). These currents were very small and rare and only seen in cell passage numbers much higher than used in this study. In contrast, we routinely observed current densities greater than 30 pA pF^{-1} in HEK cells transfected with Ca^{2+} channel cDNA. Thus, endogenous currents would contribute, at most, a very minor component of the current we observed.

The time courses depicted in the Fig. 3 show the reversibility of PnTx3-6 inhibition and provide reasonable estimates of the toxin off-rate constants. Overall, the relationship $1/\tau_{on}$ versus concentration was linear, as expected for 1:1 interaction between the channel and the toxin. The values of IC_{50} obtained by fitting the dose-response data were systematically higher than the K_d values obtained from analysis of the kinetics of blockade. However, the results from both methods agree that the toxin has highest affinity for α_{1B} channels. Binding experiments could reveal which of these two values (IC_{50} or K_d) is closer to the true disassociation constant for the interaction between toxin and channel.

The biophysical characterization of different channel isoforms has been successfully carried out using heterologous expression systems, e.g., HEK 293 cells or *Xenopus* oocytes. Whereas these systems certainly provide technical advantages, they may not fully replicate the in vivo milieu. This is evident from the fact that biophysical properties of expressed channels may differ from those seen in neurons (Sidach and Mintz, 2002). Channels formed by α_{1B} subunits are potently blocked by ω-conotoxin GVIA (Williams et al., 1992; Stea et al., 1993), as are native N-type channels (Randall and Tsien, 1995). Our results in N18 cells indicate virtually complete block of native N-type (i.e., ω-conotoxin GVIA-sensitive) Ca^{2+} channels by PnTx3-6 and partial block of the GVIA-R current in these cells. Literature data suggest L-type Ca^{2+} channels contribute to the GVIA-R component (Carlson et al., 1994), which was supported by our observation that this current was increased by BayK8644. We could not completely block the GVIA-R component with 10 μM nifedipine (not shown), which may be due to the negative holding potential used (Bean, 1984; Kokubun et al., 1986) or may indicate other channel types contributed to the GVIA-R current in our conditions. Regardless of the composition of the GVIA-R component, the data indicate that PnTx3-6 almost completely blocked the N-type, GVIA-S component, consistent with results on channels expressed in HEK cells.

PnTx3-6 Mechanism of Action. To bind to ion channels and to alter cellular function, it has been suggested that peptide toxins may act by two different mechanisms: modification of gating or pore blockade. The so-called gating modifier toxins bind close to the channel voltage sensor, and alter the voltage dependence or kinetics of gating, whereas pore-blocking toxins bind to outer mouth of the channel and physically occlude the permeation pathway (McDonough et al., 2002; Sidach and Mintz, 2002; for review, see Doering and Zamponi, 2003). It has been reported that ω-Aga-IIIA and ω-conotoxins (GVIA/MVIIC) partially or completely inhibit N-type Ca^{2+} channels through pore blockade (Mintz, 1994; McDonough et al., 1996). McDonough et al. (1996) suggest at least two distinct extracellular toxin binding site on the N-type channel and three on the P-type Ca^{2+} channel. There is some evidence that ω-agatoxin IIIA and ω-conotoxins GVIA/MVIIC bind to the same site on N- and P-type channels, possibly interacting with residues in the extracellular portion of domain III S5-S6 linker (Yan and Adams, 2000).

The broad specificity of PnTx3-6 inhibition and its blockade profile seems similar to ω-Aga-IIIA on HVA channels. Moreover, analysis of the sequence of PnTx3-6 in the Gen-

Bank database reveals some identity with the amino acid sequence of ω-Aga-IIIA and ω-Aga-IIIB (Table 1; Cordeiro et al., 1993). Although the molecular binding site of PnTx3-6 is unknown, our results suggest that PnTx3-6 acts in two different ways to occlude the external pore of the channels. For complete blockade of N-type currents by PnTx3-6, it seems that the toxin may bind tightly to the external mouth of the channel and physically occlude the pore. On the other hand, when PnTx3-6 is applied to P/Q-, L-, and R-type currents an incomplete blockade is reached, suggesting that the toxin might be too big to fit tightly within the outer vestibular of the pore, producing reduction of the conductance without eliminating the current flow. This effect would be similar to that described for the partial blockade of P/Q-type Ca^{2+} channels by the peptide ω-Aga-IIIA (McDonough et al., 2002).

In summary, we have characterized the PnTx3-6 effects on a family of neuronal Ca^{2+} channels. The toxin exhibited measurable preference for N-type channels among the HVA Ca^{2+} channel subtypes tested, and blockade of this channel type was reversible. It has been shown that blockade of N-type channels has pharmacological utility to treat pain. As an example, intrathecal injection of a synthetic version of ω-conotoxin MVIIA has been used to block pain transmission (Wang et al., 2000). Improved understanding of toxins may be an important advance in the development of therapeutic agents. Our results suggest that PnTx3-6 may block HVA Ca^{2+} channels by physically occluding the channel, and we propose that PnTx3-6 may be used as a probe to study structural differences between subtypes of HVA Ca^{2+} channels. The present results explain inhibition by this toxin of Ca^{2+} entry and Ca^{2+}-dependent glutamate release from isolated nerve terminals (Vieira et al., 2003). For this reason, we suggest this toxin be referred to in the future as ω-PnTx3-6.

Acknowledgments

We thank Dr. André Massensini for assistance with N18 cell culture. We thank Dr. Adriano Pimenta for helpful discussions.

References

Bean BP (1984) Nitrendipine block of cardiac calcium channels: high-affinity binding to the inactivated state. *Proc Natl Acad Sci USA* **81:**6388–6392.

Berjukow S, Doring F, Froschmayr M, Grabner M, Glossmann H, and Hering S (1996) Endogenous calcium channels in human embryonic kidney (HEK293) cells. *Br J Pharmacol* **118:**748–754.

Bourinet E, Charnet P, Tomlinson WJ, Stea A, Snutch TP, and Nargeot J (1994) Voltage-dependent facilitation of a neuronal alpha 1C L-type calcium channel. *EMBO (Eur Mol Biol Organ) J* **13:**5032–5039.

Carlson RO, Masco D, Brooker G, and Spiegel S (1994) Endogenous ganglioside GM1 modulates L-type calcium channel activity in N18 neuroblastoma cells. *J Neurosci* **14:**2272–2281.

Cassola AC, Jaffe H, Fales HM, Castro Afeche S, Magnoli F, and Cipolla-Neto J (1998) Omega-phonetoxin-IIA: a calcium channel blocker from the spider *Phoneutria nigriventer*. *Pflugers Arch* **436:**545–552.

Catterall WA (1995) Structure and function of voltage-gated ion channels. *Annu Rev Biochem* **64:**493–531.

Chuang RS, Jaffe H, Cribbs L, Perez-Reyes E, and Swartz KJ (1998) Inhibition of T-type voltage-gated calcium channels by a new scorpion toxin. *Nat Neurosci* **1:**668–674.

Cordeiro MN, Figueiredo SG, Valentim AC, Diniz CR, Eicksted RD, Goroy J, and Richardson M (1993) Purification and amino acid sequences of six TX3 type neurotoxins from the venom of the Brazilian "armed" spider *Phoneutria nigriventer*. *Toxicon* **31:**35–42.

Doering CJ and Zamponi GW (2003) Molecular pharmacology of high voltage-activated calcium channels. *J Bioenerg Biomembr* **35:**491–505.

Dos Santos RG, Van Renterghem C, Martin-Moutot N, Mansuelle P, Cordeiro MN, Diniz CR, Mori Y, De Lima ME, and Seagar M (2002) *Phoneutria nigriventer* omega-phonetoxin IIA blocks the Cav2 family of calcium channels and interacts with omega-conotoxin-binding sites. *J Biol Chem* **277:**13856–13862.

Dubel SJ, Starr TV, Hell J, Ahlijanian MK, Enyeart JJ, Catterall WA, and Snutch TP (1992) Molecular cloning of the alpha-1 subunit of an omega-conotoxin-sensitive calcium channel. *Proc Natl Acad Sci USA* **89:**5058–5062.

Dunlap K, Luebke JI, and Turner TJ (1995) Exocytotic Ca2+ channels in mammalian central neurons. *Trends Neurosci* **18:**89–98.

Dworakowska B and Dolowy K (2000) Ion channels-related diseases. *Acta Biochim Pol* **47:**685–703.

Feng ZP, Doering CJ, Winkfein RJ, Beedle AM, Spafford JD, and Zamponi GW (2003) Determinants of inhibition of transiently expressed voltage-gated calcium channels by omega-conotoxins GVIA and MVIIA. *J Biol Chem* **278:**20171–20178.

Gomez MV, Kalapothakis E, Guatimosin C, and Prado MA (2002) *Phoneutria nigriventer* venom: a cocktail of toxins that affect ion channels. *Cell Mol Neurobiol* **22:**579–588.

Hamill OP, Marty A, Neher E, Sakmann B, and Sigworth FJ (1981) Improved patch-clamp techniques for high-resolution current recording from cells and cell-free membrane patches. *Pflugers Arch* **391:**85–100.

Hildebrand ME, McRory JE, Snutch TP, and Stea A (2004) Mammalian voltage-gated calcium channels are potently blocked by the pyrethroid insecticide allethrin. *J Pharmacol Exp Ther* **308:**805–813.

Jen J (1999) Calcium channelopathies in the central nervous system. *Curr Opin Neurobiol* **9:**274–280.

Kobayashi T and Mori Y (1998) Ca2+ channel antagonists and neuroprotection from cerebral ischemia. *Eur J Pharmacol* **363:**1–15.

Kokubun S, Prodhom B, Becker C, Porzig H, and Reuter H (1986) Studies on Ca channels in intact cardiac cells: voltage-dependent effects and cooperative interactions of dihydropyridine enantiomers. *Mol Pharmacol* **30:**571–584.

Leão RM, Cruz JS, Diniz CR, Cordeiro MN, and Beirao PS (2000) Inhibition of neuronal high-voltage activated calcium channels by the omega-*Phoneutria nigriventer* Tx3-3 peptide toxin. *Neuropharmacology* **39:**1756–1767.

Mackie K, Devane WA, and Hille B (1993) Anandamide, an endogenous cannabinoid, inhibits calcium currents as a partial agonist in N18 neuroblastoma cells. *Mol Pharmacol* **44:**498–503.

McDonough SI, Boland LM, Mintz IM, and Bean BP (2002) Interactions among toxins that inhibit N-type and P-type calcium channels. *J Gen Physiol* **119:**313–328.

McDonough SI, Swartz KJ, Mintz IM, Boland LM, and Bean BP (1996) Inhibition of calcium channels in rat central and peripheral neurons by omega-conotoxin MVIIC. *J Neurosci* **16:**2612–2623.

McRory JE, Santi CM, Hammning KS, Mezeyova J, Sutton KG, Baillie DL, Stea A, and Snutch TP (2001) Molecular and functional characterization of a family of rat brain T-type calcium channels. *J Biol Chem* **276:**3999–4011.

Mintz IM (1994) Block of Ca channels in rat central neurons by the spider toxin omega-Aga-IIIA. *J Neurosci* **14:**2844–2853.

Newcomb R, Szoke B, Palma A, Wang G, Chen X, Hopkins W, Cong R, Miller J, Urge L, Tarczy-Hornoch K, et al. (1998) Selective peptide antagonist of the class E calcium channel from the venom of the tarantula *Hysterocrates gigas*. *Biochemistry* **37:**15353–15362.

Olivera BM, Gray WR, Zeikus R, McIntosh JM, Varga J, Rivier J, de Santos V, and Cruz LJ (1985) Peptide neurotoxins from fish-hunting cone snails. *Science (Wash DC)* **230:**1338–1343.

Randall A and Tsien RW (1995) Pharmacological dissection of multiple types of Ca2+ channel currents in rat cerebellar granule neurons. *J Neurosci* **15:**2995–3012.

Rezende LJ, Cordeiro MN, Oliveira EB, and Diniz CR (1991) Isolation of neurotoxic peptides from the venom of the 'armed' spider *Phoneutria nigriventer*. *Toxicon* **29:**1225–1233.

Schroeder CI, Smythe ML, and Lewis RJ (2004) Development of small molecules that mimic the binding of omega-conotoxins at the N-type voltage-gated calcium channel. *Mol Divers* **8:**127–134.

Sidach SS and Mintz IM (2002) Kurtoxin, a gating modifier of neuronal high- and low-threshold Ca channels. *J Neurosci* **22:**2023–2034.

Soong TW, Stea A, Hodson CD, Dubel SJ, Vincet SR, and Snutch TP (1993) Structure and functional expression of a member of the low voltage-activated calcium channel family. *Science (Wash DC)* **260:**1133–1136.

Starr TV, Prystay W, and Snutch TP (1991) Primary structure of a calcium channel that is highly expressed in the rat cerebellum. *Proc Natl Acad Sci USA* **88:**5621–5625.

Stea A, Dubel SJ, Pragnell M, Leonard JP, Campbell KP, and Snutch TP (1993) A beta-subunit normalizes the electrophysiological properties of a cloned N-type Ca2+ channel alpha 1-subunit. *Neuropharmacology* **32:**1103–1116.

Vieira LB, Kushmerick C, Reis HJ, Diniz CR, Cordeiro MN, Prado MA, Kalapothakis E, Romano-Silva MA, and Gomez MV (2003) PnTx3-6 a spider neurotoxin inhibits K+-evoked increase in [Ca2+] (i) and Ca2+-dependent glutamate release in synaptosomes. *Neurochem Int* **42:**277–282.

Wang YX, Gao D, Pettus M, Phillips C, and Bowersox SS (2000) Interactions of intrathecally administered ziconotide, a selective blocker of neuronal N-type voltage-sensitive calcium channels, with morphine on nociception in rats. *Pain* **84:**271–281.

Williams ME, Brust PF, Feldman DH, Patthi S, Simerson S, Maroufi A, McCue AF, Velicelebi G, Ellis SB, and Harpold MM (1992) Structure and functional expression of an omega-conotoxin-sensitive human N-type calcium channel. *Science (Wash DC)* **257:**389–395.

Yan L and Adams ME (2000) The spider toxin omega-Aga IIIA defines a high affinity site on neuronal high voltage-activated calcium channels. *J Biol Chem* **14:**21309–21316.

Zamponi GW, Bourinet E, Nelson D, Nargeot J, and Snutch TP (1997) Crosstalk between G proteins and protein kinase C mediated by the calcium channel alpha1 subunit. *Nature (Lond)* **385:**442–446.

Address correspondence to: Dr. Marcus Vinícius Gomez, Departamento de Farmacologia, ICB-Universidade Federal de Minas Gerais, Avenida Antonio Carlos, 6627, Belo Horizonte, MG 30270-901 Brazil. E-mail: gomez@icb.ufmg.br